

## ABSORPTION AND STATIC EMISSION PROPERTIES OF MONOMETALATED QUINONE-SUBSTITUTED PORPHYRIN DIMERS: EVIDENCE FOR "SUPEREXCHANGE" MEDIATED ELECTRON TRANSFER IN MULTICOMPONENT PHOTOSYNTHETIC MODEL SYSTEMS

Jonathan L. Sessler,\* Martin R. Johnson, and Tzu-hn-Yuan Lin

Department of Chemistry, University of Texas at Austin, Austin, TX 78712 USA

(Received in USA 2 December 1988)

### Abstract

The absorption and static emission properties of several selectively metalated quinone-substituted porphyrin dimers and control compounds are described. Whereas the unsubstituted metal-free and bis-zinc dimers 16, 19, 17, and 20 give rise to fluorescence emission spectra characteristic of typical monomeric free-base and zinc-containing porphyrins (e.g. 13 and 14), the corresponding monometalated dimers (15 and 18) display emission spectra characteristic only of free-base porphyrins, indicating that rapid exothermic energy transfer takes place between the metalated and free-base subunits in these latter systems. In the case of the control monomers, direct covalent attachment of a quinone subunit (to give 9-12) serves to quench all detectable fluorescence emission. Similar results are obtained in the case of the metal-free (3), bis-zinc (4), and "distal" monometalated materials (2) in either 2-methyl THF or toluene at room temperature. This suggests that in these systems net electron transfer from the porphyrin dimer ensemble to the quinone is fast compared to the rate of fluorescence emission. In the case of the "proximal" monometalated complex, 1, however, a weak but detectable fluorescence signal is observed when the sample is irradiated in toluene at room temperature, indicating that the built-in energy barrier provided by the "proximal" zinc porphyrin subunit is slowing the rate of net electron transfer. Nonetheless, even in the case of this system, the rate of net electron transfer remains exceedingly high, suggesting that the central or "proximal" metalated porphyrin serves to mediate the electron transfer process. The quantum yield for fluorescence for this material in 2-methyl THF is essentially temperature independent, increasing by only a factor of 3 upon cooling from room temperature to 77 K. This suggests that net electron transfer from the "distal" free-base subunit to the quinone is not thermally activated but takes place by a direct superexchange mediated process. A similar conclusion is derived from analogous studies of the "flat" compounds 5-8. Here, however, the quantum yields for fluorescence are higher throughout the series suggesting that net electron transfer is slower for these more open photosynthetic models.

### Introduction

Electron transfer (ET) reactions play a central role in biology.<sup>1-6</sup> They are a crucial component in a wide range of enzymatic processes and play an important role in both photosynthesis<sup>1,4-6</sup> and respiratory oxidative phosphorylation.<sup>6</sup> The latter process is, of course, required for aerobic metabolism, and hence, all higher life. In it, electrons are transported through a series of carriers consisting of:



Coenzyme Q and the heme protein cytochrome c are well-defined, water soluble species which serve as migrating links between the other carriers.<sup>6</sup> Unfortunately, the latter are metalloprotein aggregates with membrane bound prosthetic groups and have not yet proved amenable to X-ray structural analysis. As a result, much of our current understanding of complex *multistep* processes derives from studies of bacterial photosynthetic

reaction centers (RCs).<sup>7-9</sup> At present, the RCs are the only membrane bound ET protein for which a highly refined crystal structure exists. They thus represent our best chance to investigate and understand in detail a *multistep* biological ET reaction *in a protein*. The extensive experimental and theoretical work on RCs over the past few years reflects this point of view, as does the voluminous literature on photosynthetic model systems. This perception has been further underscored by the recent announcement of the 1988 Nobel Prize in Chemistry: It was awarded to Johann Deisenhofer, Hartmut Michel, and Robert Huber for their work in determining the X-ray crystal structure of the reaction center from *Rhodospseudomonas viridis*.<sup>7</sup>

Two RCs, those from *Rhodospseudomonas viridis*<sup>7</sup> and *Rhodobacter sphaeroides*,<sup>8,9</sup> have now been characterized structurally. Six tetrapyrrolic subunits are found at the two very similar active sites: A dimeric bacteriochlorophyll "special pair" (P), two "accessory" bacteriochlorophylls (Bchls), and two bacteriopheophytins (Bphs), all held in a well-defined but skewed geometry along a C<sub>2</sub> axis of symmetry. The Bchls are separated from P by center-to-center distances of ca. 11 Å and interplane angles of ca. 70°. The Bphs in turn are separated by similar distances and angles from the Bchls. Four of these six prosthetic groups are currently considered to define the relevant electron transport chain.<sup>5</sup> This consists in sequence of the photosensitizer (P), an "accessory" Bchl, an intermediate Bph, and a quinone acceptor (Q). In *R. sphaeroides*, Q is an ubiquinone; in *R. viridis*, it is a menaquinone. In both cases, Q lies roughly 13-14 Å away from the corresponding Bph center. Charge separation between P<sup>\*</sup> and Bph entities is known to occur on a time scale of 2-4 ps with nearly 100% quantum efficiency.<sup>10-13</sup> Furthermore this process exhibits activationless behavior, increasing in rate by a factor of two at liquid helium temperature.<sup>10,14</sup> The resulting P<sup>+</sup>-Bchl-Bph<sup>-</sup> charge separated state can exist stably for a long period of time; in the normal course of events *in vivo*, a subsequent electron transfer to give P<sup>+</sup>-Bchl-Bph-Q<sup>-</sup> occurs in 200 ps, also with 100% quantum yield.<sup>5</sup>

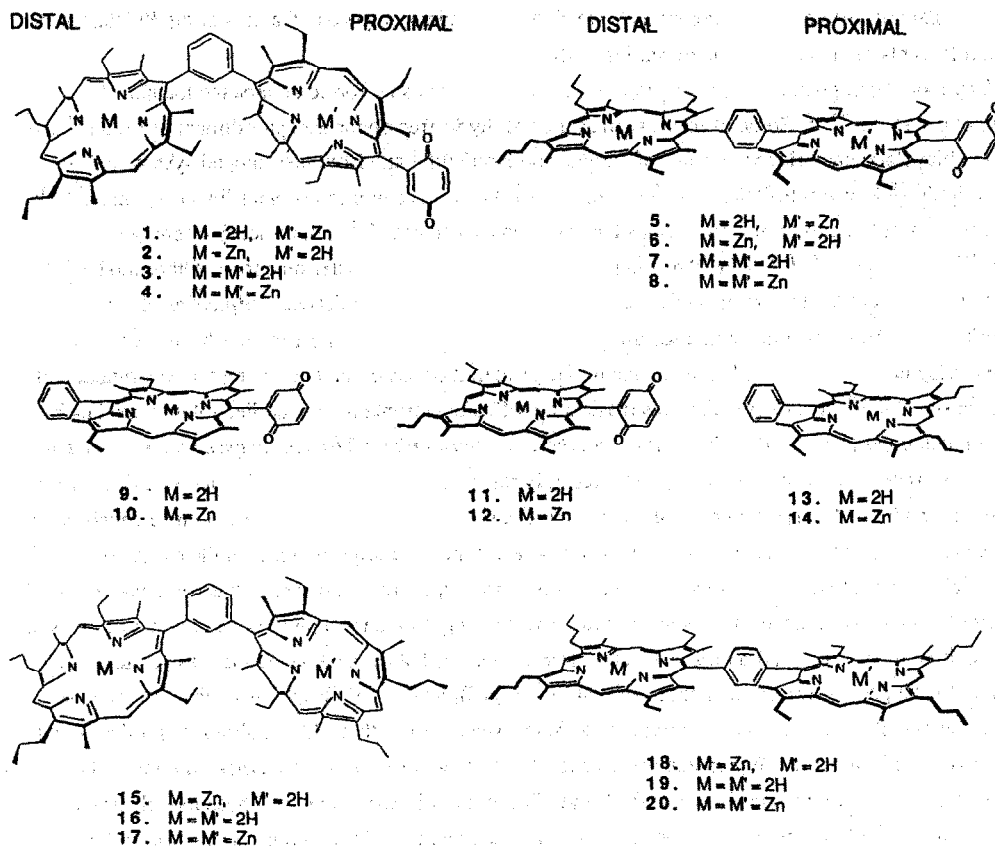
In spite of the availability of the above structural and kinetic data, many aspects of bacterial photosynthesis, including the rapid, activationless, and efficient nature of the initial charge separation process, remain poorly understood.<sup>1,4,5</sup> One of the more crucial questions currently being debated is the role of the "intermediate" or "accessory" Bchl. Recent subpicosecond transient absorption experiments have failed to provide any evidence that a P<sup>+</sup>-Bchl<sup>-</sup> state acts as a discrete intermediate in the initial P<sup>\*</sup>-Bchl-Bph → P<sup>+</sup>-Bchl-Bph<sup>-</sup> charge separation process.<sup>10-13</sup> Nonetheless, it seems unlikely that the electron traverses the ca. 17 Å center-to-center distance from the P to the Bph in a few ps without the Bchl prosthetic group playing an important role. An attractive but as yet unproven possibility is that the Bchl facilitates transfer to the Bph via a "superexchange" mechanism involving a quantum mechanical mixing of a virtual P<sup>+</sup>-Bchl<sup>-</sup> state with the photoexcited dimer, P<sup>\*</sup>.<sup>15-17</sup> There has been a great deal of controversy (but no definitive resolution) as to whether or not such a mechanism is consistent with other experimental observations, e.g. the small singlet-triplet splitting of the radical pair state formed upon charge separation.<sup>16,18</sup> Critical as the "superexchange" question is, it is important to realize that many other issues remain unresolved. For example, how important are chromophore orientations in controlling the ET rates? Why does charge separation proceed primarily down one branch of the approximate C<sub>2</sub> axis? What is the precise role of the protein? How can one explain the relatively weak temperature dependence, the extremely slow back reactions, and the high quantum yield? Currently great efforts are being made to modify the natural system (e.g., via prosthetic group replacement,<sup>19</sup> site directed mutagenesis,<sup>20</sup> or by applying a large electric field<sup>21</sup>) and thus examining some of these questions more systematically. Nonetheless, there are fundamental limitations at present in our ability to manipulate such

a complicated natural system. Model compounds which actually mimic important features of the RC thus have a valuable role to play in unraveling the mysteries of RC function.

Many model compounds have been prepared in recent years in an effort to understand the natural photosynthetic systems.<sup>22-44</sup> Some of these, such as the porphyrin-free donor-acceptor dimers of Miller<sup>23</sup> and others,<sup>24</sup> the bicyclooctane bridged systems of Dervan and Hopfield<sup>25</sup> and Bolton,<sup>26</sup> capped systems of Staab,<sup>27</sup> Dolphin,<sup>28</sup> Mauzerall,<sup>29</sup> Sanders,<sup>30</sup> and others,<sup>31,32</sup> as well as numerous other linked systems,<sup>23,33-35</sup> have proved useful in exploring how various factors, such as distance,<sup>25-31</sup> donor-acceptor energetics,<sup>25c,30,35b</sup> and solvent,<sup>26,30,33,34b,35b</sup> mediate photoinduced electron transfer reactions. Other models,<sup>36-38</sup> such as the triads and related systems of Gust and Moore<sup>36</sup> and triptycene-derived porphyrins of Wasielewski,<sup>37</sup> exhibit interesting charge separation properties. By and large these studies have been very informative; they have, for instance led to the unambiguous identification of an inverted region as a function of driving force,<sup>23,25c,30b,37</sup> an effect which was masked by diffusional limitations in earlier solution studies.<sup>45</sup> Nonetheless, it is important to realize that *in all cases there are substantial differences between the models and the actual RCs*. Indeed, with the exception of two recently reported quinone-substituted metal-free dimers,<sup>39,40</sup> (and our own work<sup>41-44</sup> discussed below), *all* photosynthetic model systems reported to date have consisted of a simple *monomeric* porphyrin substituted with one or more acceptors. Furthermore, with the exception of our own work, only one photosynthetic model system, the quinone-capped system of Staab, has been characterized structurally.<sup>27b</sup> As a result, model studies have so far provided only limited insight into the critical questions of interchromophore interactions and multistep electron transfer outlined above and have failed, as yet, to provide much useful mechanistic information about the initial  $SP^+ \text{-Bchl-Bphe} \rightarrow SP^+ \text{-Bchl-Bphe}^-$  charge separation process. Given the obvious importance, however, of these issues, we felt that additional model studies would be informative. We have therefore prepared and characterized a new series of photosynthetic models: The selectively metalated, quinone-substituted "gable" and "flat" dimers **1**, **2**, **5**, and **6**.<sup>42</sup> These models provide the first "matched set" of photosynthetic models suitable for studying interchromophore orientation and energetic effects in biomimetic systems, and, in the case of **1** and **5**, provide the first examples wherein possible porphyrin-based superexchange mediated charge separation processes might be observed in synthetic systems. In this paper we present the results of static fluorescence quenching studies which are consistent with apparent superexchange behavior in **1** and **5**; the results of corroborative femtosecond transient absorption spectroscopic studies are the subject of a separate report.<sup>43</sup>

### Design Considerations

An essential feature of compounds **1**, **2**, **5**, and **6** is that they possess a well-defined conformational structure. In other words they are not "floppy". Initial estimates of the intersubunit orientations and distances could therefore be obtained from CPK space filling molecular models. The center-to-center distances between the unsubstituted "distal" porphyrin ( $MP_d$ ) and the quinone were estimated to be 14 Å in the gable series and 20 Å in the flat compounds. Similarly, the center-to-center distances between the distal and "proximal" ( $MP_p$ ) porphyrin subunits were estimated to be 10.5 Å and 12.5 Å in the gable and flat series respectively. Studies of CPK models also suggested that in both the gable and flat systems the flanking methyl substituents at positions 3 and 7 force the porphyrins to adopt a conformation that is perpendicular to the bridging phenyl subunits. Moreover, for the same type of reason, the quinone was expected to lie perpendicular to the proximal



porphyrin. The available X-ray structural data, the full details of which will be presented elsewhere,<sup>44</sup> are consistent with these predictions. A single crystal X-ray diffraction study of the monomeric free-base quinone **11** has now been completed; it shows that the quinone makes an angle of  $84^\circ$  with the porphyrin core, and reveals a center-to-center distance of  $6.5 \text{ \AA}$  between the porphyrin and quinone subunits (Figure 1). Preliminary X-ray structural information is also available for the biscopper(II) chelates of the symmetrically substituted bis-dimethoxyphenyl-derivitized analogues of **16** and **19** (Figures 2 and 3). These structures confirm the predicted porphyrin center-to-center distances: The intramolecular Cu-Cu separations are  $10.5 \text{ \AA}$  and  $12.7 \text{ \AA}$  for the gable and flat systems respectively. These structures also reveal several other interesting structural features. For instance, in the flat dimer, the two porphyrin macrocycles are found to be essentially coplanar and perpendicular to the bridging phenyl ring. In the case of the 1,3-phenyl linked system, on the other hand, the two porphyrin subunits help define what can be considered an overall "skewed" arrangement contained within the context of a gable-type configuration. The obvious structural similarity between this synthetic structure and parts of the RC (notably the Bchl and Bph pair) is a feature we consider to be of particular interest.

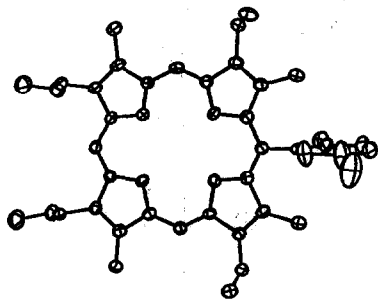


Figure 1

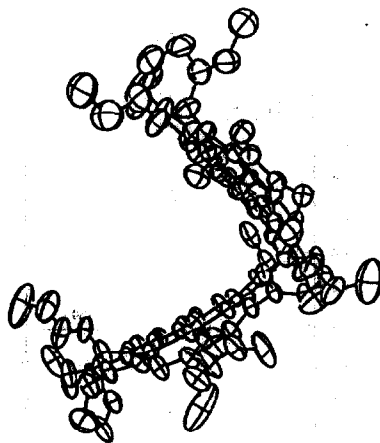


Figure 2

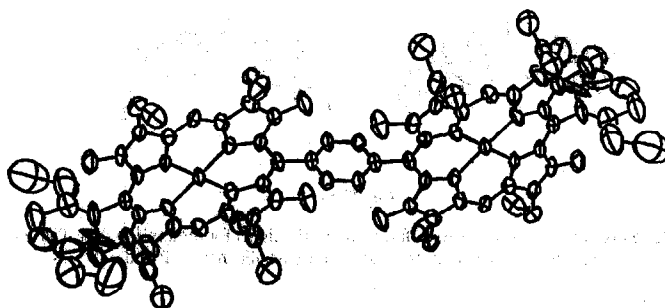


Figure 3

A second unusual feature of the selectively monometalated compounds **1**, **2**, **5**, and **6** is that the relative subunit energetics are controlled. In these systems, the lowest excited singlet state of the zinc(II) porphyrin subunit lies ca. 0.17 eV higher in energy than that of the corresponding free-base system.<sup>42</sup> As a result, two different energetic arrangements are defined for each regioisomeric pair **1** and **5**, and **2** and **6**. This is illustrated schematically in Figure 4 which shows the ground and excited state redox potentials for compounds **1** and **2**. In compound **2** (and **6**), an energy gradient exists for net electron transfer from the photoexcited distal porphyrin,  $\text{ZnP}_d^*$ , through the proximal subunit  $\text{H}_2\text{P}_p^*$  (or  $\text{H}_2\text{P}_p^-$ ), to the quinone acceptor Q (Figure 4, frame A). In model **1** (and **5**), on the other hand, the proximal  $\text{ZnP}_p$  porphyrin defines an energy barrier between the photoexcited distal subunit  $\text{H}_2\text{P}_d^*$  and Q (Figure 4, frame B). Systems **1** and **5** thus represent the first photosynthetic models that mimic the apparent energetic arrangement of the P-Bchl-Bph RC chromophores.

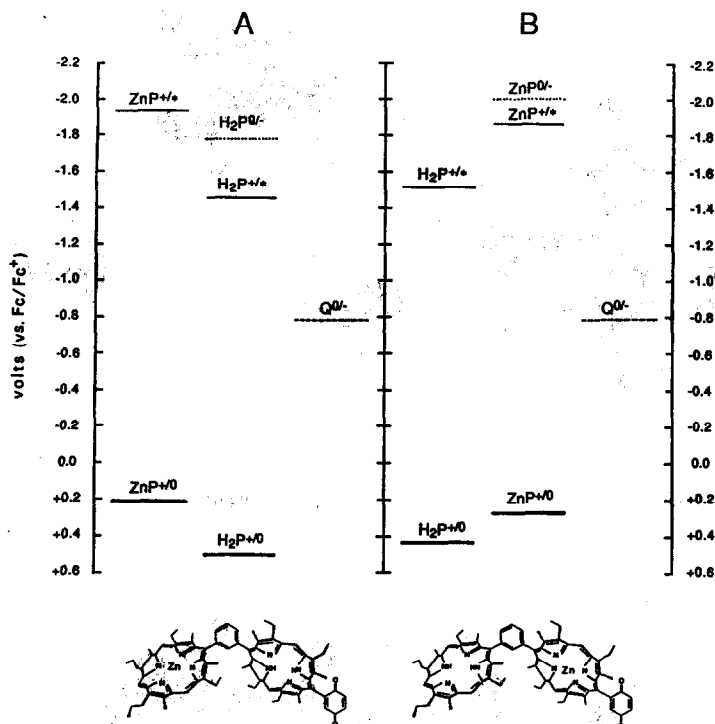


Figure 4.

Ground and excited state redox potentials (volts versus ferrocene/ferricinium) for dimers 1 and 2. These data are taken from reference 42 where further explanatory details may be found.

### Absorption Spectra

The electronic spectra of the dimeric systems 1-8 and 15-20 suggest that the two porphyrin-chromophores do not act as entirely independent light absorbing entities. Rather, as has been observed in other rigidly linked porphyrin dimers,<sup>41, 46-49</sup> all of these compounds show evidence of optical coupling as revealed by split, broadened, and/or shifted Soret bands. This coupling is most apparent in the case of the gable-type bis-zinc complexes 4 and 17. For instance, while the control monomer 10 shows only one sharp Soret band at 414 nm, the Soret of the gable dimer 4 is split into two peaks of nearly equal intensity at 407 and 424 nm (Figure 5). In addition, the dimer 4 displays a molar absorptivity that is roughly twice that of the monomer 9, in keeping with the greater number of chromophores per molecule. The bis-zinc flat dimers also show evidence for excitonic interaction: Compound 8, for instance, shows a single strong Soret peak ( $\lambda_{\text{max}} = 424$  nm) that is red-shifted by 10 nm relative to 10 and displays only a slight shoulder at higher energy ( $\lambda_{\text{max}} = 412$  nm) (Figure 5). The origins of these splittings are well known and have been discussed in detail by other workers;<sup>48</sup> they are *not* due to the presence of the quinone substituent. In the case of the free-base dimers 3, 7, 16 and

19, no detectable splitting of the Soret band is observed. Rather, these transitions are broadened relative to either the appropriate control monomer or the corresponding flat compound (c.f. e.g. Figure 6). Finally, the monometalated complexes, 1, 2, 5, 6, 15, and 18, display absorption behavior which is intermediate between that of the metal-free and bis-zinc materials. This is illustrated in Figure 7 which shows the absorption spectra for the isomeric complexes 1 and 2. Interestingly, for these monometalated materials only three detectable signals are observed in the visible, or Q-band, region of the spectrum.

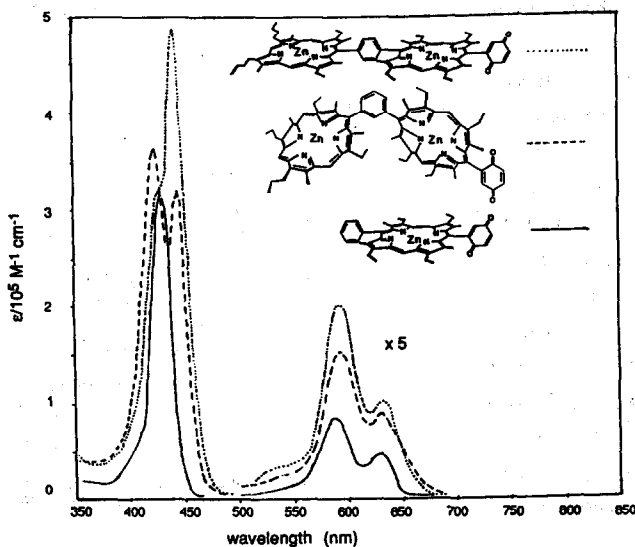


Figure 5.

Absorption spectra of bis-zinc complexes of quinone-substituted porphyrin monomers and dimers in  $\text{CHCl}_3$ .

### Excited State Properties of Quinone-free Systems

Before considering the excited state optical properties of the quinone-containing dimeric models 1-8, it is instructive to consider those of the quinone-free dimers 15-20. Irradiation of the bis-zinc complexes 17 and 20 at the Soret maximum (or in the blue region of the visible bands) gives rise to near normal zinc porphyrin emission bands (such as those observed for monomer 14) that are only slightly reduced in intensity (Table 1). Similarly, irradiation of 16 and 19 gives rise to typical free-base emission spectra, e.g. that of 13 (Figures 8 and 9). On the other hand, irradiation of the monozinc complexes 15 and 18 gives rise to strong emission bands, the wavelength of which are characteristic *only* of the free-base subunit (c.f. e.g. Figure 9). This important observation implies, as has been suggested for other loosely-linked monometalated dimers,<sup>49</sup> that exothermic energy transfer ( $-\Delta G \approx 0.17$  eV) takes place rapidly between the two porphyrin subunits. From the ratio of emission intensities at 595 nm, it is estimated that this process occurs on a subpicosecond time scale.

Direct fluorescence lifetime measurements also support the contention that rapid energy transfer takes place between the porphyrin subunits in dimers **15** and **18**. Table 1 lists the measured lifetimes of these complexes and various appropriate control compounds. All show monoexponential decays, indicative of direct radiative quenching of a single excited state. The monozinc compound **15**, for instance, displays a fluorescence lifetime of 8.8 ns, close to the 9.2 ns lifetime observed for the free-base system **16**. Similarly, compound **18**, displays a fluorescence lifetime of 10.2 ns, essentially the same within experimental error as that of its corresponding free-base **19** (9.9 ns). By contrast, the biszinc compounds **17** and **20** both display fluorescence lifetimes of ca. 2.2 ns. If energy transfer were not rapid in the monozinc complexes, two decays, with lifetimes of 2 ns and 10 ns respectively, would be expected, reflecting independent deactivation of the two different (zinc and free-base) excited state components. It should be noted, of course, that due to the close prox-

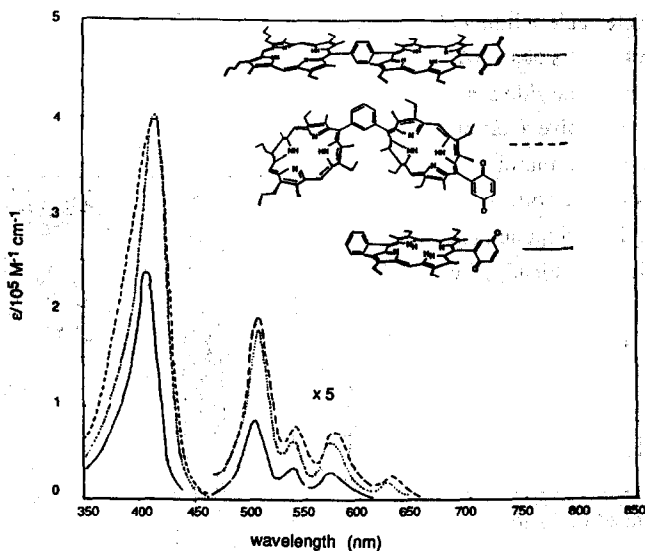


Figure 6.

Absorption spectra of metal-free quinone-substituted porphyrin monomers and dimers in  $\text{CHCl}_3$ .

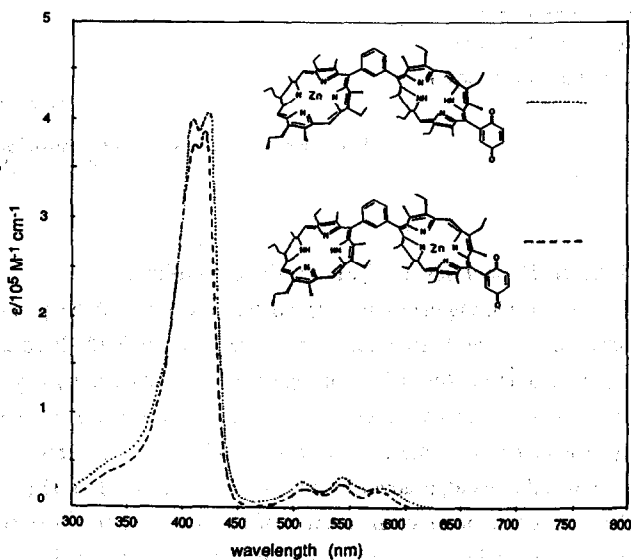


Figure 7.

Absorption spectra of monozinc complexes of quinone-substituted gable-type porphyrin dimers in  $\text{CHCl}_3$ .



imity of these values, resolution of the kinetic traces into two discrete components might not necessarily be anticipated. Nonetheless, biexponential-type behavior would be expected for photo-excited systems **15** and **18**, behavior that is *not* observed experimentally. Thus, the presence of a single exponential decay is taken as strong evidence for rapid intersubunit energy transfer in these monometalated systems.

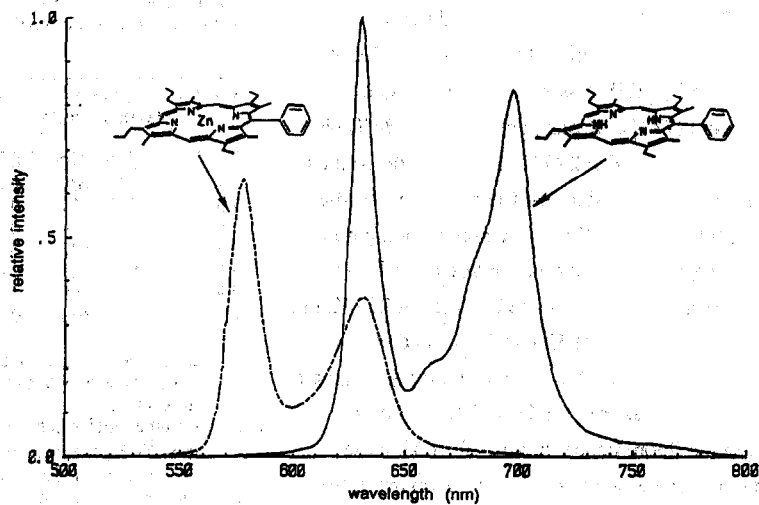


Figure 8.

Emission spectra of quinone-free porphyrin monomers in toluene at 295 K.

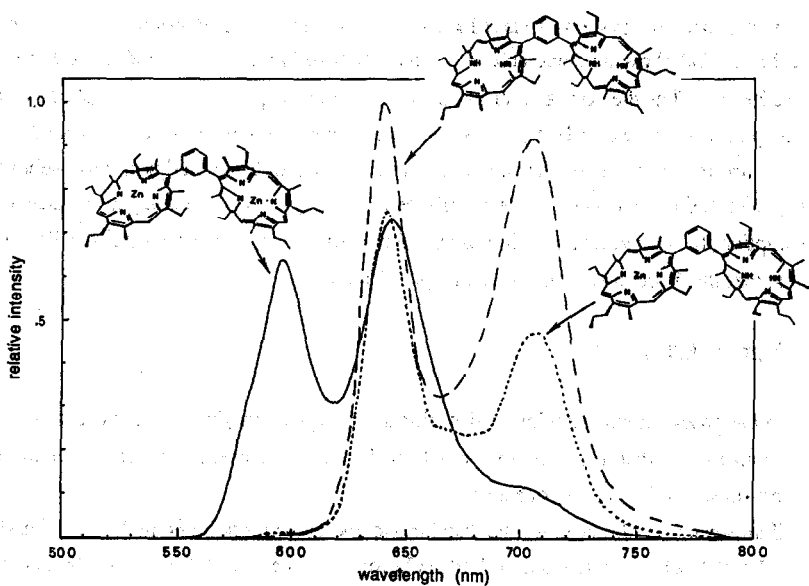


Figure 9.

Emission spectra of metal-free, monozinc, and bis-zinc gable-type porphyrin dimers in toluene at 295 K.

Studies of these quinone-free dimers were also performed in 2-methyl THF solution at 295 K and in 2-methyl THF glasses at liquid nitrogen temperature (77 K). Results are also given in Table 1. In 2-methyl THF at 295 K, the gable compounds **16** and **15** displayed identical fluorescence lifetimes (8.7 vs. 8.6 ns, respectively). Upon immersion in liquid nitrogen, these lifetimes increased to 15.3 and 14.8 ns, respectively. In 2-methyl THF at 295 K, the fluorescence lifetime of **19** was 9.8 ns and the lifetime of **18** was 11.2 ns, somewhat longer than the free-base. As was true for **15** and **16**, in liquid nitrogen the fluorescence lifetimes for both these compounds increased to ca. 15 ns. In contrast, the biszinc dimers **17** and **20** displayed short lifetimes (ca. 2 ns) in 2-methyl THF at 295 K and showed little temperature dependence.

Table 1. Emission Properties of Unsubstituted Monomeric and Dimeric Porphyrins.

Comp'd	Emission Maxima (nm) <sup>a</sup>		$\Phi_F^b$	$\tau_F^c$	$\tau_F^d$	$\tau_F^e$
<b>13</b>	630	697	0.15			
<b>14</b>	577	630	0.053			
<b>15</b>	643	707	0.070	8.8	8.6	14.8
<b>16</b>	640	704	0.075	9.2	8.7	15.3
<b>17</b>	595	643	0.046	2.2	2.0	2.1
<b>18</b>	633	701	0.079	10.2	11.2	15.0
<b>19</b>	633	699	0.091	9.9	9.8	15.5
<b>20</b>	585	639	0.043	2.2	2.0	2.2

- Measured in dilute solutions ( $< 5 \times 10^{-7}$  M) of equal optical density with excitation at the Soret maximum.
- Quantum yields in toluene at room temperature measured relative to H<sub>2</sub>TPP (tetraphenylporphyrin) ( $\Phi_F = 0.11$ ).<sup>50</sup> We estimate an uncertainty of  $\pm 10\%$  for these values.
- Fluorescence lifetime (ns) recorded in toluene solution at room temperature.
- Fluorescence lifetime (ns) recorded in 2-methyl THF solution at room temperature.
- Fluorescence lifetime (ns) recorded in 2-methyl THF glass at 77 K.

### Fluorescence Properties of Quinone-containing Systems

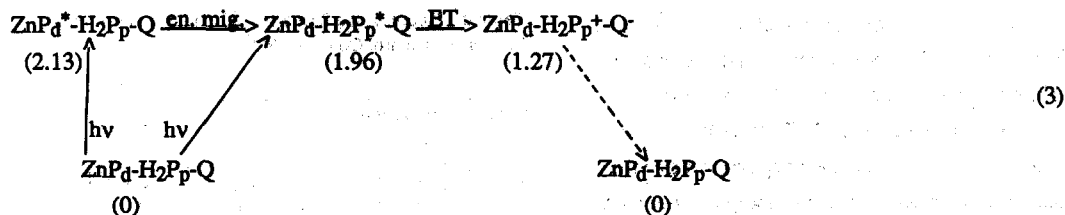
In contrast to the quinone-free systems **13** and **14**, the quinone-substituted monomeric control compounds **9** and **10** (and **11** and **12**) show no detectable emission ( $\Phi_F \leq 10^{-5}$ ) when irradiated at the Soret maximum in toluene at 295 K. Thus the normally strong fluorescence of the porphyrin chromophore is completely quenched by the presence of the covalently linked quinone acceptor. On the basis of considerable precedent,<sup>51</sup> this result is ascribed to rapid exothermic electron transfer from the excited porphyrin subunit to the adjacent quinone ( $-\Delta G \cong 0.69$  and  $1.03$  eV for **9** and **10**, respectively). Standard analyses (which are predicated on the assumption that all reduction in fluorescence intensity is due to electron transfer),<sup>25a</sup> carried out using eq. 2, suggest that this is occurring in less than 1 ps (Table 2).

$$k_{E.T.} = I_0/\tau_0 - 1/\tau_0 \quad (2)$$

Here  $I_0$  and  $\tau_0$  represent the observed emission intensities (fluorescence quantum yields) and measured fluorescence lifetimes for the control (unsubstituted) monomers **13** and **14**, and  $I$  represents the observed emission intensity for the quinone-substituted system in question.

No detectable fluorescence is observed for the distal monozinc gable monoquinone **2**, or the free-base and bis-zinc analogues **3** and **4**, when irradiated as a dilute solutions in toluene at 295 K. This absence of emission may be readily understood in terms of the control experiments described above and the energetic arrangements of the chromophores: For all three systems rapid energy transfer is possible between the porphyrin subunits in the overall direction of the quinone. Fast photoinduced charge separation may therefore take place either by rapid exoergic energy migration followed by fast electron transfer, or, in the more trivial case, by direct excitation of the proximal subunit and subsequent electron transfer. It is not surprising therefore that

no detectable emission is observed for these systems: Net electron transfer from the photoexcited dimer to the quinone acceptor is simply fast compared to the rate of fluorescence emission. This is illustrated in eq. 3 for the specific case of **2**. Here, the values in parentheses represent the state energies (in eV) of the species in question in  $\text{CH}_2\text{Cl}_2$ , derived from the data given in Figure 4, uncorrected for any possible coulombic or solvent effects.



Qualitatively, the flat distal monozinc monoquinone, the flat metal-free, and flat bis-zinc compounds **6-8** have the same energetic arrangements as the corresponding gable analogues. It is not surprising therefore that substantial fluorescence quenching is also observed for these systems. In contrast to the gable materials, however, slight but detectable fluorescence signals are observed in this series. This is presumably the result of the farther distance and/or less favorable chromophoric interactions which pertain in the flat systems. Importantly, the observed fluorescence signals are always characteristic of the distal subunit (c.f. Figure 10). This

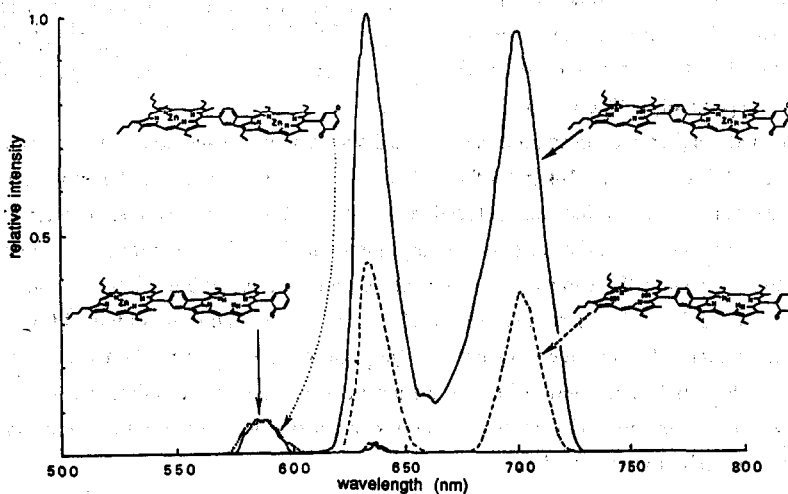


Figure 10.

Emission spectra of quinone-substituted flat-type porphyrin dimers in toluene at 295 K.

implies that the rate of excited distal porphyrin subunit deactivation by net electron transfer to the quinone is no longer "infinitely" fast compared to the rate of fluorescence. Thus, as expected on the basis of the mechanism presented in eq. 3, some distal subunit emission is therefore observed. Table 2 gives a listing of the quantum yields for these systems and the corresponding net electron transfer quenching rates derived using eq. 2. Here, the values of  $I_0$  and  $\tau_0$  refer to the emission intensities and lifetimes of either the unsubstituted (quinone-free) free-base or bis-zinc controls **19** or **20**, as appropriate.

The proximal monometalated complexes **1** and **5** differ substantially from the systems discussed so far: The energetic arrangement of the chromophores in these systems creates a ca. 0.17 eV barrier for net electron transfer from the distal porphyrin ring to the quinone via a thermally activated energy transfer pathway. As shown in Figure 4, frame B, this barrier is defined by the proximal zinc-chelated ring (ZnP<sub>p</sub>). Not surprisingly, these systems display excited state behavior that is markedly different from the systems discussed above and, indeed, from all other photosynthetic models reported to date. This is apparent in both the static fluorescence studies presented here, as well as in the femtosecond transient absorption measurements discussed in a separate report.<sup>43</sup>

Both compound **1** and **5** show modest but detectable fluorescence emission from the distal free-base subunit in toluene at room temperature ( $\Phi_F = 1.7 \times 10^{-4}$  and  $7.7 \times 10^{-4}$  respectively). These emission intensities are substantially higher than those observed for the distal monometalated complexes or the corresponding bis-zinc or metal free materials **2-4** and **6-8** (Table 2). Indeed, compound **1** is the only member of the quinone-substituted gable series to show any detectable emission. Moreover, the emission intensity observed for **2** is the highest of any of the flat series of photosynthetic models. From the ratio of emission intensities of **1** and **5** relative to **16** and **19**, respectively, net electron transfer rates of  $5.4 \times 10^{10} \text{ s}^{-1}$  and  $1.1 \times 10^{10} \text{ s}^{-1}$  ( $k_{ET}$ ) may be derived for **1** and **5**. These rates are ca. 100 times slower than those obtained for **2** and **6**. This indicates that the presence of a central energy barrier (ZnP<sub>p</sub>) slows down the rate of charge separation. These data also support the conclusion given earlier that the net electron transfer rates are noticeably slower for the more open flat systems. Thus both unfavorable orientations and energetics can serve to slow the rates of electron transfer in a series of congruent models.

Important as the above conclusions are, it is critical to realize that the net electron transfer rates for **1** and **5** are still exceedingly fast. For instance, the  $k_{ET}$  value for **5** is *over 2000 times faster than that observed for a bisbicyclooctane-derived model prepared by Joran et al.* (compound H<sub>2</sub>P<sub>2</sub>Q in Table 2),<sup>25a</sup> wherein the free-base porphyrin-to-quinone separation approximates the H<sub>2</sub>P<sub>d</sub> to Q distance found in **5**. Clearly direct through space (or through solvent) electron transfer is *not* the dominant photochemical quenching pathway in systems **1**

Table 2. Fluorescence Properties of Quinone-substituted Dimers and Control Compounds.<sup>a</sup>

Comp'd	Emission Maxima (nm)		$\Phi_F^b$	$k_{ET} \text{ (s}^{-1}\text{)}^c$
<b>1</b>	642	705	$1.7 \times 10^{-4}$	$5.4 \times 10^{10}$
<b>2</b>	d	d	$\leq 1 \times 10^{-5}$	$\geq 10^{12}$
<b>3</b>	d	d	$\leq 1 \times 10^{-5}$	$\geq 7.5 \times 10^{11}$
<b>4</b>	d	d	$\leq 1 \times 10^{-5}$	$\geq 10^{12}$
<b>5</b>	632	702	$7.7 \times 10^{-4}$	$1.1 \times 10^{10}$
<b>6</b>	587	637	$3.5 \times 10^{-5}$	$\approx 10^{12}$
<b>7</b>	632	701	$3.9 \times 10^{-4}$	$2.2 \times 10^{10}$
<b>8</b>	585	636	$2.3 \times 10^{-5}$	$\geq 10^{12}$
<b>9</b>	d	d	$\leq 1 \times 10^{-5}$	$\geq 7.5 \times 10^{11}$
<b>10</b>	d	d	$\leq 1 \times 10^{-5}$	$\geq 10^{12}$
H <sub>2</sub> P <sub>2</sub> Q <sup>e</sup>				$4 \times 10^6$

- Measured at room temperature in dilute toluene solutions with excitation at the Soret maximum.
- Quantum yields were measured relative to H<sub>2</sub>TPP ( $\Phi_F$  0.11).<sup>50</sup> Estimated uncertainty:  $\pm 10\%$ .
- Estimated using eq. 2 using the lifetime and quantum yield values for **16**, **17**, **19**, and **20** given in Table 1.
- Emission for these samples could not be detected.
- Obtained by fluorescence quenching (reference 25a).

and 5. Rather, charge separation is mediated by the central (or proximal) metalloporphyrin. This does not appear to occur via a thermally activated process: The quantum yields for fluorescence (in 2-methyl THF) of 1 and 5 increase by factors of 2 and 3, respectively upon cooling the samples from room temperature to 77 K (c.f. Figure 11); an increase of almost  $10^3$  (corresponding to a  $10^8$  decrease in net electron transfer rate) would be expected for a simple Arrhenius-type process with an analogous 0.17 eV barrier. This critical result rules out a simple two-step charge separation mechanism (analogous to that of eq. 3), involving endoergic energy transfer (from  $H_2P^*$  to  $ZnP$ ) followed by exoergic electron transfer (from  $ZnP^*$  to Q). Rather, electron transfer from  $H_2P_d^*$  to Q is apparently taking place by a direct superexchange process mediated by the proximal  $ZnP_p$  moiety. This is shown schematically in eq. 4 for the specific case of 1.

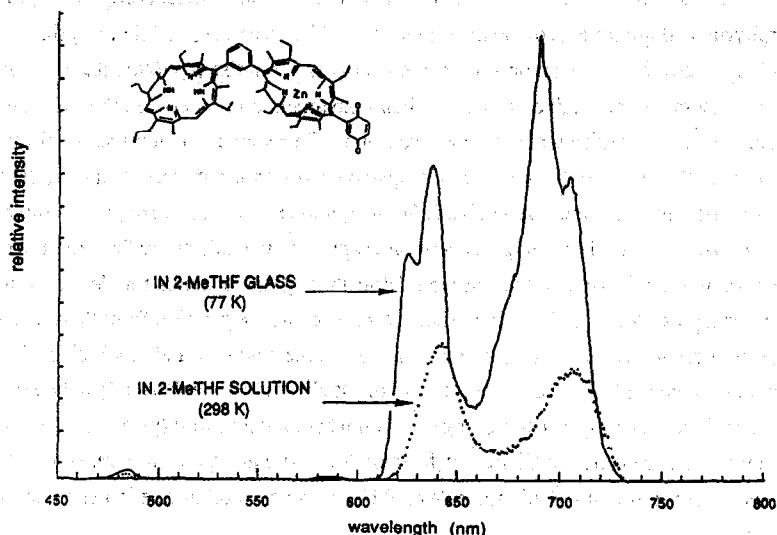
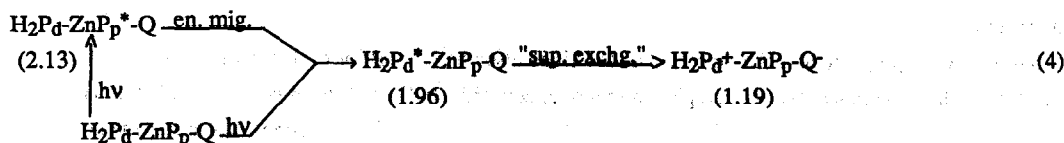


Figure 11.

Emission spectra of selectively monometalated "proximal" quinone-substituted gable-type porphyrin dimers in 2-methyl THF.



Here, the excited distal free-base subunit ( $H_2P_d^*$ ) could arise from both direct photoexcitation and rapid, exothermic energy transfer from  $ZnP_p^*$ . Once formed, the charge separated state  $H_2P_d^+-ZnP_p-Q^-$  presumably returns to the ground state by a series of nonradiative processes. Although not determined by the current experiments, we consider it likely on the basis of energetics that this process occurs by hole migration (to give  $H_2P_d-ZnP_p^+-Q^-$ ), followed by simple charge recombination. Further investigation of this matter is currently in progress.

## Conclusion

Compounds 1-2 and 5-6, which contain the key biomimetic components, metalloporphyrin, free-base porphyrin, and quinone, provide an unprecedented "matched set" of photosynthetic models suitable for studying intermacrocycle orientation and energetic effects in multistep photoinduced electron transfer reactions. These dimers do not act like the sum of their constituent monomers. Rather, all show very low emission intensities when irradiated at the Soret maximum. This suggests that rapid net electron transfer quenching takes place from the dimer to the quinone. Comparisons to simpler photosynthetic model systems indicate that net electron transfer from the distal subunit (to the quinone) is not occurring by a simple through space or through solvent pathway. Rather, charge separation is apparently mediated by the central (or proximal) porphyrin subunit. In the case of 2 and 6, a straight "downhill" gradient exists for electron transfer from the distal zinc porphyrin photodonor to the quinone acceptor and charge separation from this excited subunit proceeds via energy migration followed by electron transfer. In the case of 1 and 5, which contain a built-in energy barrier, temperature dependent fluorescence quenching studies rule out a thermally activated process. Instead, they are consistent with a charge separation mechanism wherein the central (proximal) zinc porphyrin acts as an effective superexchange mediator for the overall photoinduced electron transfer. Our findings thus support recent suggestions that a Bchl molecule could be playing a similar role in the natural photosynthetic reaction centers.

## Experimental

Steady-state fluorescence spectra were taken on a SPEX FLUOROLOG 2 equipped with a Hamamatsu IP-21 photomultiplier tube and a "datamate" workstation, and were stored on an HP-85 using the "tra spex" program supplied by the Webber group at U.T. Austin. To prevent product decomposition, the fore slit was kept no wider than 1.25 mm. The aft slit was allowed to be as wide as 5 mm. The "right angle" mode of the spectrophotometer was used for all data collection. Photomultiplier voltage settings were as follows: For the measurements in toluene,  $S_1 = 900$  volts and  $S_2 = 350$  volts; for the 2-methyl THF measurements,  $S_1 = 1000$  volts and  $S_2 = 400$  volts. Measurements at 77 K were performed with the use of a quartz Dewar flask supplied by the Webber group and appropriate supporting equipment to insure a light-tight fit. Dry  $N_2$  gas was blown into the spectrophotometer housing to prevent frosting of the Dewar flask.

Samples were prepared and characterized as described elsewhere.<sup>44</sup> Prior to fluorescence emission or lifetime studies, the quinone-containing samples were reoxidized with DDQ and repurified by careful chromatography on silica gel followed by recrystallization from chloroform-hexanes. For measurements in toluene no special precautions were required: Solutions measuring  $0.200 \pm 0.002$  A.U. were made up using dry toluene (freshly distilled from NaK alloy), placed in a 1 cm quartz fluorescence cell, and measured within one hour. Measurements involving the quinone-substituted porphyrins in 2-methyl THF, however, required careful handling to insure that the prepared solutions did not come into contact with the outside air. (Such an event inevitably resulted in a rapid increase in fluorescence with time, ascribed to contamination with water, which was found by independent experiment to lead to rapid hydroquinone formation.) All solutions were therefore prepared using dry 2-methyl THF (freshly distilled from NaK alloy) and calibrated to between 0.2 and 0.3 A.U. at the Soret maximum in an inert atmosphere "dry box" capable of sustaining an atmosphere of  $\leq 1$  ppm  $H_2O$  (or  $O_2$ ). Special 25 cm quartz probes, made from 0.8 cm o.d. x 5 cm length square quartz tubing and

blown onto a 0.3 cm. o.d. round quartz filler tube, were filled in the dry box with an elongated Pasteur pipette and sealed with the aid of a wooden applicator tightly wrapped with parafilm to achieve as airtight a seal as possible. Samples were then measured as rapidly as possible and in all cases within one hour of preparation.

A typical data collection went as follows: Up to seven identical spectra of the same sample were recorded, averaged and corrected using the datamate "COR" command. Where appropriate, the sample was then cooled and the process repeated. The sample was then carefully warmed from the top down to prevent breakage of the cell, and another measurement was made to determine the extent of quinone reduction. If the fluorescence was substantially greater than before cooling, the results of the experiment were discounted and a new sample was prepared and the process repeated. In any case, all results cited here are the result of at least three independent measurements from at least two independently prepared and purified samples.

Nanosecond lifetimes were measured by Drs. Steve Atherton and Stefan Hubig at the Center for Fast Kinetic Research, University of Texas at Austin using using a Hamamatsu streak camera. The setup was configured as described earlier<sup>52</sup> with the exception that a 532 nm, 30 ps (fwhm) pulse from a Quantel YG 402 laser was used as the excitation source. Errors in these measurements are considered to be less than  $\pm 10\%$ .

### Acknowledgments

This work was supported by the Robert A. Welch Foundation (grant F-1018 to J.L.S.), the National Science Foundation (PYI Award, 1986 to J.L.S.), the Camille and Henry Dreyfus Foundation (New Faculty Award, 1984 to J.L.S.), and the National Institutes of Health (grant no. HL 131572 to J.A.I.). We thank Prof. S. Webber for use of his fluorometer and the staff at the Center for Fast Kinetics Research at the University of Texas at Austin (an NIH supported shared user facility) for help in recording fluorescence lifetimes. J.L.S. thanks Profs. R. Friesner and D. Holten for helpful discussions.

### References

1. Marcus, R. A.; Sutin, N. *Biochim. Biophys. Acta* **1985**, *810*, 265-322.
2. Guarr, T.; McLendon, G. *Coord. Chem. Rev.* **1985**, *68*, 1-52.
3. Scott, R. A.; Mauk, A. G.; Gray, H. B. *J. Chem. Ed.* **1985**, 932-937.
4. Windsor, M. W. *J. Chem. Soc., Faraday Trans. 2* **1986**, 2237-2243.
5. Kirmaier, C.; Holten, D. *Photosyn. Res.* **1987**, *13*, 225-260.
6. Stryer, L. *Biochemistry, 2nd Ed.*, Freeman, San Francisco, 1975.
7. (a) Deisenhofer, J.; Epp, O.; Miki, K.; Huber, R.; Michel, H. *J. Mol. Biol.* **1984**, *180*, 385-398; (b) Deisenhofer, J.; Epp, O.; Miki, K.; Huber, R.; Michel, H. *Nature*, **1985**, *318*, 618-624.
8. Chang, C.-H.; Tiede, D.; Tang, J.; Smith, U.; Norris, J.; Schiffer, M. *FEBS Lett.* **1986**, *205*, 82-86.
9. (a) Allen, J. P.; Feher, G.; Yeates, T. O.; Rees, D. C.; Deisenhofer, J.; Michel, H.; Huber, R. *Proc. Natl. Acad. Sci. USA* **1986**, *83*, 8589-8593; (b) Allen, J. P.; Feher, G.; Yeates, T. O.; Komiya, H.; Rees, D. C. *Proc. Natl. Acad. Sci. USA* **1987**, *84*, 5730-5734.
10. Woodbury, N. W.; Becker, M.; Middendorf, D.; Parson, W. W. *Biochemistry* **1985**, *24*, 7516-7521.
11. (a) Martin, J.-L.; Breton, J.; Hoff, A. J.; Migus, A.; Antonetti, A. *Proc. Natl. Acad. Sci. USA* **1986**, *83*, 957-961; (b) Breton, J.; Martin, J. L.; Migus, A.; Antonetti, A.; Orszag, A. *Proc. Natl. Acad. Sci. USA* **1986**, *83*, 5121-5125.

12. Wasielewski, M. R.; D. M. Tiede, D. M. *FEBS Lett.* **1986**, *204*, 368-372.
13. Kirmaier, C.; Holten, D. *FEBS Lett.* **1988**, in press.
14. Fleming, G. R., J. L. Martin and J. Breton (1988) *Nature (London)* **333**, 190-192.
15. (a) Ogrodnik, A.; Remy-Richter, N.; Michel-Beyerle, M. E. *Chem. Phys. Lett.* **1987**, *135*, 576-581; (b) Bixon, M.; Jortner, J.; Michel-Beyerle, M. E.; Orgodnik, A.; Lersch, W. *Chem. Phys. Lett.* **1987**, *140*, 626-630; (c) Plato, M.; Möbius, K.; Michel-Beyerle, M. E.; Bixon, M.; Jortner, J. *J. Am. Chem. Soc.* **1988**, *110*, 7279-7285.
16. Marcus, R. A. *Chem. Phys. Lett.* **1987**, *133*, 471-476.
17. (a) Won, Y.; Friesner, R. A. *Proc. Natl. Acad. Sci. U.S.A.* **1987**, *84*, 5511-5515; (b) Won, Y.; Friesner, R. A. *Biochim. Biophys. Acta* **1988**, *975*, 9-18.
18. Boxer, S. G.; Chidsey, C. E. D.; Roelofs, M. G. *Ann. Rev. Phys. Chem.* **1983**, *34*, 389-417.
19. Gunner, M. R.; Robertson, D. E.; Dutton, P. L. *J. Phys. Chem.* **1986**, *90*, 3783-3795.
20. Holten, D.; Kirmaier, C. *Abstracts of 196<sup>th</sup> ACS Meeting, Los Angeles, California, September 25-30, 1988*.
21. (a) Lockhart, D. J.; Boxer, S. G. *Biochemistry*, **1987**, *26*, 664-668.
22. For reviews of early work see: (a) Fendler, J. H. *J. Phys. Chem.* **1985**, *89*, 2730-2740; (b) Boxer, S. G. *Biochim. Biophys. Acta*, **1983**, *726*, 265-292.
23. (a) Miller, J. R.; Calcaterra, T. L.; Closs, G. L. *J. Am. Chem. Soc.* **1984**, *106*, 3047-3049; (b) Miller, J. R.; Beitz, J. V.; Huddleston R. K. *J. Am. Chem. Soc.* **1984**, *106*, 5057-5068; (c) Closs, G. L.; Calcaterra, T. L.; Gree, N. J.; Penfield, K. W.; Miller, J. R. *J. Phys. Chem.* **1986**, *90*, 3673-3683; (d) Penfield, K. W.; Miller, J. R.; Paddon-Row, M. N.; Cotsaris, E.; Oliver, A. M.; Hush, N. S. *J. Am. Chem. Soc.* **1987**, *109*, 5061-5065; (e) Closs, G. L.; Piotrowiak, P.; MacInnis, J. M.; Fleming, G. R. *J. Am. Chem. Soc.* **1988**, *110*, 2652-2653; (f) Closs, G. L.; Miller, J. R. *Science* **1988**, *240*, 440-447.
24. (a) Warman, J. M.; De Haas, M. P.; Oevering, H.; Verhoeven J. W.; Paddon-Row, Oliver, A. M.; Hush, N. S. *Chem. Phys. Lett.* **1986**, *128*, 95-99; (b) Pasman, P.; Rob, F.; Verhoeven, J. W. *J. Am. Chem. Soc.* **1982**, *104*, 5127-5133.
25. (a) Joran, A. D.; Leland, B. A.; Geller, G. G.; Hopfield, J. J.; Dervan, P. B. *J. Am. Chem. Soc.* **1984**, *106*, 6090-6092; (b) Leland, B. A.; Joran, A. D.; Felker, P. M.; Hopfield, J. J.; Zewail, A. H.; Dervan, P. B. *J. Phys. Chem.* **1985**, *89*, 5571-5573; (c) Joran, A. D.; Leland, B. A.; Felker, P. M.; Zewail, A. H.; Hopfield, J. J.; Dervan, P. B. *Nature (London)* **1987**, *327*, 508-511.
26. Bolton, J. R.; Ho, T.-F.; Liauw, S.; Siemiarczuk, A.; Wan, C. S. K.; Weedon, A. C. *J. Chem. Soc., Chem. Commun.* **1985**, 559-560.
27. (a) Weiser, J.; Staab, H. A. *Angew. Chem. Int. Ed. Engl.* **1984**, *23*, 623-625; (b) Krieger, C.; Weiser, J.; Staab, H. A. *Tetrahedron Lett.* **1985**, 6055-6058; (c) Weiser, J.; Staab, H. A. *Tetrahedron Lett.* **1985**, 6059-6063.
28. Morgan, B.; Dolphin, D. *Angew. Chem. Int. Ed. Engl.* **1985**, *24*, 1003-1004.
29. Lindsey, J. S.; Mauzerall, D. C. *J. Am. Chem. Soc.* **1982**, *104*, 4498-4500; (b) Lindsey, J. S.; Mauzerall, D. C. *J. Am. Chem. Soc.* **1983**, *105*, 6528-6529; (c) Lindsey, J. S.; Delaney, J. K.; Mauzerall, D. C.; Linschitz, H. *J. Am. Chem. Soc.* **1988**, *110*, 3610-3621.



30. (a) Leighton, P.; Sanders, J. K. M. *J. Chem. Soc., Chem. Commun.* **1985**, 24-25; (b) Irvine, M. P.; Harrison, R. J.; Beddard, G. S.; Leighton, P.; Sanders, J. K. M. *Chem. Phys.* **1986**, *104*, 315-324; (c) Harrison, R. J.; Pearce, B.; Beddard, G.S.; Cowan, J. A.; Sanders, J. K. M. *Chem. Phys.* **1987**, *116*, 439-448.
31. Osuka, A.; Furuta, H.; Maruyama, K. *Chem. Lett.* **1986**, 479-482.
32. Sanders, G. M.; van Dijk, M.; van Veldhuizen, A.; van der Plas, H. C. *J. Chem. Soc., Chem. Commun.* **1986**, 1311-1316.
33. (a) Siemiarzuck, A.; McIntosh, A. R.; Ho, T.-F.; Stillman, M. J.; Roach, K. J.; Weedon, A. C.; Bolton, J. R.; Connolly, J. S. *J. Am. Chem. Soc.* **1983**, *105*, 7224-7230; (b) Schmidt, J. A.; Siemiarzuck, A.; Weedon, A. C.; Bolton, J. R. *J. Am. Chem. Soc.* **1985**, *107*, 6112-6114; (c) Schmidt, J. A.; McIntosh, A. R.; Weedon, A. C.; Bolton, J. R.; Connolly, J. S.; Hurley, J. K.; Wasielewski, M. R. *J. Am. Chem. Soc.* **1988**, *110*, 1733-1740.
34. (a) Migita, M.; Okada, T.; Mataga, N.; Nishitani, S.; Kurata, N.; Sakata, Y.; Misumi, S. *Chem. Phys. Lett.* **1981**, *84*, 263-266; (b) Mataga, N.; Karen, A.; Okada, T.; Nishitani, S.; Kurata, N.; Sakata, Y.; Misumi, S. *J. Phys. Chem.* **1984**, *88*, 5138-5141.
35. (a) Wasielewski, M. R.; Niemczyk, M. P. *J. Am. Chem. Soc.* **1984**, *106*, 5043-5045; (b) Wasielewski, M. R.; Niemczyk, M. P.; Svec, W. A.; Pewitt, E. B. *J. Am. Chem. Soc.* **1985**, *107*, 1080-1082.
36. (a) Moore, T. A.; Gust, D.; Mathis, P.; Mialocq, J.-C.; Chachaty, C.; Bensasson, R. V.; Landl, E. J.; Doizi, D.; Liddell, P. A.; Lehman, W. R.; Nemeth, G. A.; Moore, A. L. *Nature (London)* **1984**, *307*, 630-632; (b) Liddell, P. A.; Barrett, D.; Makings, L. R.; Pessiki, P. J.; Gust, D.; Moore, T. A. *J. Am. Chem. Soc.* **1986**, *108*, 5350-5352; (c) Gust, D.; Moore, T. A.; Liddell, P. A.; Nemeth, G. A.; Makings, L. A.; Moore, A. L.; Barrett, D.; Pessiki, P. J.; Bensasson, R. V.; Rougee, M.; Chachaty, C.; De Schryver, F. C.; Van der Auweraer, M.; Holzwarth, A. R.; Connolly, J. S. *J. Am. Chem. Soc.* **1987**, *109*, 846-856; (d) Gust, D.; Moore, T. A.; Moore, A. L.; Barrett, D.; Harding, L. O.; Makings, L. R.; Liddell, P. A.; De Schryver, F. C.; Van der Auweraer, M.; Bensasson, R. V.; Rougee, M. *J. Am. Chem. Soc.* **1988**, *110*, 321-323, and references therein.
37. Wasielewski, M. R.; Niemczyk, M. P.; Svec, W. A.; Pewitt, E. B. *J. Am. Chem. Soc.* **1985**, *107*, 5562-5563.
38. Nishitani, S.; Kurata, N.; Sakata, Y.; Karen, A.; Okada, T.; Mataga, N. *J. Am. Chem. Soc.* **1983**, *105*, 7771-7772.
39. Sakata, Y.; Nishitani, S.; Nishimizu, N.; Misumi, S.; McIntosh, A. R.; Bolton, J. R.; Kanda, Y.; Karen, A.; Okada, T.; Mataga, N. *Tetrahedron Lett.* **1985**, 5207-5210.
40. Cowan, J. A.; Sanders, J. K. M.; Beddard, G. S.; Harrison, R. J. *J. Chem. Soc., Chem. Commun.* **1987**, 55-58.
41. (a) Sessler, J. L.; Johnson, M. R. *Angew. Chem. Int. Ed. Engl.* **1987**, *26*, 678-680; (b) Sessler, J. L.; Piering, S. *Tetrahedron Lett.* **1987**, 6569-6573.
42. Sessler, J. L.; Johnson, M. R.; Lin, T.-Y.; Creager, S. E. *J. Am. Chem. Soc.* **1988**, *110*, 3659-3661.
43. Sessler, J. L.; Rodriguez, J.; Kirmaier, C.; Johnson, M. R.; Creager, S. E.; Holten, D. *J. Am. Chem. Soc.*, submitted.

44. Sessler, J. L.; Johnson, M. R.; Ibers, J. A.; Fettingner, J., manuscript in preparation.
45. See for instance: (a) Taube, H. in *Tunnelling in Biological Systems*, Chance, B. et al. eds., Academic Press, New York, 1979; (b) Weller, A. *Z. Phys. Chem.* **1982**, *133*, 93-98.
46. Heiler, D.; McLendon, G.; Rogalskyj, P. *J. Am. Chem. Soc.* **1987**, *109*, 604-606.
47. (a) Tabushi, I.; Sasaki, T. *Tetrahedron Lett.* **1982**, 1913-1916. (b) Tabushi, I.; Kugimiya, S.-I.; Kinnaird, M. G.; Sasaki, T. *J. Am. Chem. Soc.* **1985**, *107*, 4192-4199.
48. (a) Osuka, A.; Maruyama, K. *Chem. Lett.* **1987**, 825-828; (b) Osuka, A.; Maruyama, K. *J. Am. Chem. Soc.* **1988**, *110*, 4454-4456.
49. See for instance: (a) Schwarz, F. P.; Gouterman, M.; Muljiani, Z.; Dolphin, D. *Bioinorg. Chem.* **1972**, *2*, 1-32. (b) Anton, J. A.; Loach, P. A.; Govindjee *Photochem. Photobiol.* **1978**, *28*, 235-242. (c) Mialocq, J. C.; Giannotti, C.; Maillard, P.; Momenteau, M. *Chem. Phys. Lett.* **1984**, *112*, 87-93. (d) Brookfield, R. L.; Ellul, H.; Harriman, A.; Porter, G. *J. Chem. Soc., Faraday Trans. 2* **1986**, *82*, 219-233.
50. Gouterman, M. in *The Porphyrins*, Dolphin, D., Ed.; Academic: New York, 1978; Vol. III, chapter 1.
51. See for example: (a) Bergkamp, M. A.; Dalton, J.; Netzel, T. L. *J. Am. Chem. Soc.* **1982**, *104*, 253-259. (b) Mataga, N.; Karen, A.; Okada, T.; Nishitani, S.; Kurata, Sakata, Y.; Misumi, S. *J. Phys. Chem.* **1984**, *88*, 5138-5141.
52. Rodgers, M. A. *J. Chem. Phys. Lett.* **1981**, *78*, 509-514.